Journal Pre-proof

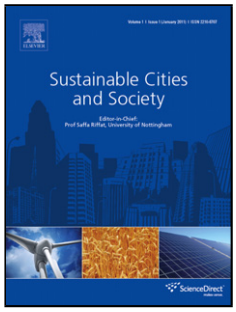

Impacts of roundabouts in suburban areas on congestion-specific vehicle speed profiles, pollutant and noise emissions: An empirical analysis

P. Fernandes, R. Tomas, F. Acuto, A. Pascale, B. Bahmankhah, C. Guarnaccia, A. Granà, M.C. Coelho

PII: S2210-6707(20)30607-7

DOI: https://doi.org/10.1016/j.scs.2020.102386

Reference: SCS 102386

To appear in: *Sustainable Cities and Society*

Received Date: 22 November 2019

Revised Date: 7 July 2020

Accepted Date: 8 July 2020

Please cite this article as: Fernandes P, Tomas R, Acuto F, Pascale A, Bahmankhah B, Guarnaccia C, Granà A, Coelho MC, Impacts of roundabouts in suburban areas on congestion-specific vehicle speed profiles, pollutant and noise emissions: An empirical analysis, *Sustainable Cities and Society* (2020), doi: https://doi.org/10.1016/j.scs.2020.102386

Impacts of roundabouts in suburban areas on congestion-specific vehicle speed profiles, pollutant and noise emissions: An empirical analysis

Fernandes P. [a*], Tomas, R. [a], Acuto, F. [b], Pascale, A. [a], Bahmankhah, B. [a], Guarnaccia, C. [c], Granà, A. [b], Coelho, M.C. [a]

[a] Department of Mechanical Engineering / Centre for Mechanical Technology and Automation (TEMA), University of Aveiro, Campus Universitário de Santiago, 3810-193 Aveiro – Portugal

[b] Department of Engineering, University of Palermo, Piazza Marina, 61, 90133 Palermo PA

[c] Department of Engineering, University of Palermo, viale delle Scienze Ed 8, 90128 Palermo, Italy

[*]Assistant Researcher, Mechanical Engineering, E-mail: paulo.fernandes@ua.pt

Highlights

- Suburban single-lane, compact two-lane and multi-lane roundabouts were assessed
- Field acoustic, tailpipe emissions, traffic, and congestion data were collected
- Predictive discrete choice models for speed profiles occurrence were developed
- Single-lane had the lowest CO_2 per vehicle, but it resulted in high noise levels

ABSTRACT

Increasing concern about global warming and air quality has meant an increasing use of energetic and environmental indicators in roundabout design. This research compares different suburban roundabouts in terms of traffic performance, pollutant and noise emissions through an integrated empirical assessment. Field measurements were carried out with a light duty vehicle in single-lane (SL), compact two-lane (CTL) and multi-lane (ML) roundabouts using Portable Emission Measurements Systems, OBD scan tool and Sound Level Meter, to measure real-world exhaust emissions, engine activity and acoustic data, respectively. Afterwards, predictive discrete choice models that correlate the probability of occurrence of speed profiles (no stop, stop once and multiple stops) with roundabout operational parameters were developed. Although SL yielded the lowest CO_2 per vehicle, a high equivalent continuous A-weighted sound level (L_{Aeq}) was returned because vehicles drove at moderate speeds in the approach and low conflicting traffic was identified when compared to the other layouts. CTL was the worst option in terms of both CO_2 and NO_X. The proposed methodology can be used to quantify the performance of roundabout layouts in suburban areas by simply identifying their traffic volumes, noise level, pollutant emission and representative speed profiles. This can help researchers, traffic planners or practitioners to reduce congestion and emissions, and enhance road traffic management near urban areas.

Keywords: Roundabouts, Speed Profiles, Discrete Models, On-road Emissions, Noise.

1. INTRODUCTION AND RESEARCH OBJECTIVES

The fast growth of cities in the past few decades has prompted an unprecedented number of vehicles and complex network infrastructure**.** According to the European Environment Agency, carbon dioxide (CO_2) emissions from road traffic have been rising consecutively

since 2013 **(EEA, 2019)**. Along with climate change, environmental pollution has become a matter of concern in the past decade, with an increasing number of acute air pollution episodes **(WHO, 2016)**. Almost 20 and 54 million people living close to rural and urban roads, respectively, in EU-28, were exposed to average night-time noise levels exceeding 50 dBA **(EEA, 2018)**. The effects of traffic noise on human health can be either physiological (e.g., a long term exposure to road traffic noise is detrimental to hearing, thus causing cardiovascular, nervous and endocrine problems) or psychological (e.g., prompting intense feelings such as disappointment, anxiety, anger and annoyance) **(Yuan et al., 2019a)**.

The amount of exhaust gases and noise emitted by motor vehicles depend on speed profile, vehicle type, traffic volumes, road and pavement features, and intersections **(Meneguzzer et al., 2017; Sandberg, 1987)**, being the latter commonly recognized as noise and pollution hotspots locations **(Covaciu et al., 2015; Fernandes et al., 2015)** due to considerable speed changes cycles in their vicinity **(Can and Aumond, 2018; Chauhan et al., 2018).**

Roundabouts have been considered around the world to replace stop-controlled junctions as a means of improving operational and safety performance. Roundabout is typically suggested as traffic control treatment at intersections with balanced traffic volumes between major and minor legs, low percentage of through traffic, more than four legs, or irregular layout **(Rodegerdts et al., 2007; Rodegerdts et al., 2010)**. Their design forces drivers to slow down and decelerate as they approach the roundabout and steering laterally around the central island and accelerate as they exit the circulating traffic **(Fernandes et al., 2016)**. Roundabout operation is impacted by the volumes of entry and conflicting flows that, in situations of congestion, can result in long queues upstream and

blockage in the circulating area **(Coelho et al., 2006; Fernandes et al., 2016; Salamati et al., 2013)**.

Despite the demonstrated safety benefits, traffic flow improvements and reduction of vehicle delay **(Park et al., 2018)**, some configurations of roundabouts raise some doubts concerning pollutants and noise emissions **(Fernandes et al., 2016; Fernandes et al., 2018; Vasconcelos et al., 2014)**. There has been increasing interest among traffic planners and engineers in building different roundabout layouts to take advantage of the operational and safety benefits. Thus, any model capable of estimating those traffic externalities, and concurrently accounting for location-specific needs is paramount of interest.

Roundabouts can be used as a strategy of access road traffic management near urban areas **(Rodegerdts et al., 2010)**. Roundabouts in suburban areas typically combine features of both urban and rural environments. On the one side, they can include pedestrian and bicycle features and small inscribed circle diameters. On the other side, suburban roundabouts can present high approaching speeds and thus may require special attention to visibility and cross-sectional details **(Rodegerdts et al., 2010)**.

There are six different categories of roundabouts according to their size, number of lanes and demand **(Brilon, 2014; Rodegerdts et al., 2010)**. Among these, single-lane (SL), multi-lane (ML) and compact-two lane (CTL) have been popular and adopted in many European countries and in the United States (US). SL has typically inscribed circle diameters (ICD) between 27 and 55 meters, and it includes raised central island treatment, truck apron, crosswalks, and single-lane entries and exits. ML is characterized as having two-lane entries and exits, and ICD values ranging from 46 to 91 meters. Lastly, CTL has ICD values up to 60 meters, at least one two-lane entry and single lane exits only. SL,

ML and CTL can handle daily service traffic volumes up to 25 000, 45 000 and 32 000 vehicles, respectively **(Rodegerdts et al., 2010).**

Although these roundabouts have different dimensions (even for the same layout) and approaching speeds, the capacity mechanisms are often analogous: one entry lane and two lanes on the ring (CTL); one entry lane and one lane on the ring (SL) and; two entry lanes and two lanes on the ring (ML). This capacity mechanism can have an impact on the overall performance of roundabouts. For instance, if SL is located in a suburban environment and exhibits high approach speeds at the entry and on the circulatory roadway, then SL may present lower traffic congestion and emissions levels, and concurrently higher noise than CTL or ML.

Bearing this in mind, this paper quantifies and contrasts on-road pollutants emissions and noise levels produced by road traffic in different types of suburban roundabouts. It was hypothesized that CO_2 and nitrogen oxides (NO_X) emissions, and equivalent continuous A-weighted sound level (L_{Aeq}) are impacted by the differences in: *1*) the approaching, conflicting and exiting traffic volumes; *2*) the V/C ratio; and *3*) the roundabout design features: SL, CTL and ML.

Field measurements of acoustic data, traffic and congestion levels were carried out in roundabouts installed at suburban roads to predict the probability of speed trajectory profiles – no stop (SPI), one-stop (SPII) and multiple stops (SPIII). On-road emissions were also collected from a light duty vehicle (LDV) using an integrated portable emissions measurement system (iPEMS). To compare several operational scenarios, **Quartieri et al. (2010)** models were employed to estimate traffic noise.

Therefore, the contributions of the study may be valuable for the following reasons:

1. One of the first studies that address and compare the real-world pollutants and noise emissions on different types of roundabouts simultaneously. Most of the existing studies often use microscopic traffic simulation tools that, per se, cannot wholly characterize driving behavior and traffic operations without robust and often time-consuming calibration techniques;
2. The development of a method that incorporates operational characteristics and environmental variables in an integrated way. In this case, the adoption of a discrete choice model capable of identifying the three speed profiles (no stop, one stop and multiple stops) using location and variability parameters of the observations taken at roundabouts. This provides not only evidence-based information on transportation stakeholders (e.g., traffic planners and authorities, local authorities) for urban design and planning but also contributes to the sustainability of the population living close to city centers.

The paper is organized into five sections. **Section 2** offers a review of the literature relevant to this paper. **Section 3** discusses the materials and methods used, while **section 4** presents and discusses the main results of the developed work. The last section describes the conclusions, limitations of the study and scope for future work.

2. LITERATURE REVIEW

Research of impacts of roundabouts in different built environments on pollutant emissions and noise in different locations are summarized in the next sections. For each section there are two main groups: the first, which makes up most of the studies,

established their results through models, while the second group, used only empirical data.

2.1. Pollutant Emissions

One of the most widely applied method is the Vehicle Specific Power (VSP) that uses on-road emission data from PEMS and is a function of vehicle speed, road grade, and acceleration **(Frey et al., 2008; US EPA, 2002)**. A good deal of research has documented the great effectiveness of the VSP methodology to estimate the emissions of vehicles at SL **(Coelho et al., 2006; Vasconcelos et al., 2014)**, CTL **(Fernandes and Coelho, 2019)**, ML **(Fernandes et al., 2016; Salamati et al., 2013; Vasconcelos et al., 2014)** and turbo roundabouts **(Fernandes et al., 2017b)**. One of the first studies on this topic was performed by **Coelho et al. (2006)**. They used a hybrid approach based on field data for vehicle activity and VSP. Results showed that vehicles at a roundabout follow one of three possible trajectories: *i*) vehicle travels through the roundabout by slowing down in response to the geometrics without stopping; or *ii*) vehicle comes to a complete stop at the yield line to negotiate a gap in the circulating ring; and *iii*) vehicle enters a queue and faces stop-and-go situations until passing the yield line. They also found that the occurrence of these profiles depended on the entry and conflicting traffic flows **(Coelho et al., 2006)**. The extension of this research methodology covers multi-lane roundabouts in Portugal **(Fernandes et al., 2016; Salamati et al., 2013)** and in the United States **(Salamati et al., 2015)**, and turbo-roundabouts without curb raised dividers in Spain **(Fernandes et al., 2016)**. Nevertheless, these studies used emission data gathered from passenger cars under US conditions.

Even though research has been conducted in light duty cars using PEMS under a wide range of road and operating conditions **[e.g. (Mahesh et al., 2018; Pouresmaeili et al.,**

2018)], few studies using PEMS can be found in different roundabout layouts. Existing research in this field has dealt with the comparison of roundabouts and other traffic control treatments such as traffic lights **(Gastaldi et al., 2017; Hallmark et al., 2011; Liu et al., 2017; Meneguzzer et al., 2018; Meneguzzer et al., 2017)** and stop-controlled intersections **(Hallmark et al., 2011)**. The findings were not clear about the emission benefits of roundabouts. **The research of Hallmark et al. (2011)** evidenced that, under uncongested conditions and depending on the driving style, type of pollutant, traffic and intersection characteristics, a roundabout can perform worse than a stop-controlled intersection, or signalized intersection on a same arterial. Conversely**, Gastaldi et al. (2017)** showed a signal-controlled intersection replaced by a CTL resulted in less CO_2 emissions. **Meneguzzer et al. (2017)** focused on emission benefits posed by the conversion of a signalized intersection to CTL. The results obtained were mixed: roundabouts produced less CO_2 emissions in almost all tested conditions; and traffic lights yielded lower NO_X emissions for all scenarios.

PEMS has also been used to explore the relationship between exhaust emissions and vehicle operating modes at a roundabout. An on-road pilot emission test was conducted by **Liu et al. (2017)** in a SL located in Houston, Texas. They found that a 35 km/h approaching speed minimized the CO_2 emissions.

In a recent study by **Jaworski et al. (2019)**, the authors undertook the assessment of exhaust emissions at four conventional two-lane roundabouts and one turbo-roundabout. They created emission models for CO_2, total hydrocarbons (THC), carbon monoxides (CO) and NO_X for various types of passenger vehicles and fuels **(Jaworski et al., 2019)**. **Fernandes et al. (2019)** have developed models for CO_2 and NO_X emissions based on internally observable variables from four light duty diesel vehicles (LDDV) on urban and

rural routes composed of several CTL and ML. However, the specific impacts of the roundabout layout on route emissions were not explored.

2.2. Traffic Noise

Steady-state calculation **[e.g., (Givargis and Mahmoodi, 2008; Kephalopoulos et al., 2014; Makarewicz and Kokowski, 2007; Rochat and Fleming, 2002; Sakamoto, 2015)]** and dynamic simulation **[e.g., (Luo et al., 2012; Ramírez and Domínguez, 2013; Wang et al., 2017)]** are widely-used models for traffic noise prediction. The first models are based on aggregated kinematic information such as road traffic volumes and average speeds **(Garg and Maji, 2014)**, while the second ones use microscopic information of vehicle activity data, namely the relative position of vehicle/receiver, speed and acceleration **(Guarnaccia, 2013).**

Research on traffic noise prediction near roundabouts has been conducted, and the above-mentioned approaches have been used for traffic noise characterization at roundabouts **(Chevallier et al., 2009; Covaciu et al., 2015; Estévez-Mauriz and Forssén, 2018; Gardziejczyk and Motylewicz, 2016; Guarnaccia, 2010; Li et al., 2017; Makarewicz and Golebiewski, 2007; To and Chan, 2000). To and Chan (2000)** developed an analytical solution of the noise level at any distance from the center of a roundabout, but the developed equation was only tested under particular traffic conditions. **Guarnaccia (2010)** presented a study of intersections noise modeling by means of noise mapping software, comparing the existing standard cross intersection configuration with a possible roundabout. The results confirmed that the roundabout configuration produces a reduction in noise levels of about 1 dBA. **Covaciu et al. (2015)** used noise mapping software LIMA to produce noise contours of three traffic control treatments (signalized intersection with the same and reduced speeds and roundabout). Other studies compared

traffic noise between signalized intersections and roundabouts **(Chevallier et al., 2009; Li et al., 2017; Makarewicz and Golebiewski, 2007)**. They found that roundabouts resulted in lower sound levels. However, **Estévez-Mauriz and Forssén (2018)** confirmed that L_{Aeq} at an unsignalized crossing near a ML can be higher than a signalized crossing. **Gardziejczyk and Motylewicz (2016)** also obtained higher values of noise in signalized roundabouts in comparison to classical channelized intersections with signalization. They also emphasized that noise levels at signalized roundabouts must consider the traffic management and vehicle types at individual entries and sub-intersection **(Gardziejczyk and Motylewicz, 2016).**

Interest has increased in the past few years in using road traffic noise models for multi-criteria approaches. **Fernandes et al. (2017a)** used a genetic algorithm to optimize vehicle delay, emissions, pedestrian travel time, and overall source power level emitted under different crosswalk locations in relation to the circulatory ring of ML. **Fernandes et al. (2018)** modeled emissions and noise impacts of partial-metering strategies at a rural corridor with three ML and one SL. The system, which was designed to reduce external emission (CO_2 and NO_X) and noise costs, resulted in improvements up to 13% compared to the unmetered conditions.

2.3. Summary gaps

Although pollutants and noise emissions in roundabouts, as well as their comparison with other traffic control treatments, have been well explored, there are some gaps observed in the prior studies:

- Little attention has been paid about the environmental and noise performance of roundabouts installed at suburban environments;

- There is no robust comparison of different emission and noise impacts among roundabouts with different layouts (generally focus on the comparison between roundabouts and other traffic control-treatments);
- Research did not explore in detail the impact of entry lanes and developed speed trajectories profiles that account for capacity, global and local pollutant emissions and noise impacts of roundabouts in an integrated way.

3. METHODOLOGY

The research team collected experimental data on noise, vehicle exhaust emissions, dynamic and engine, as well as overall congestion levels in through movements from three roundabouts in Aveiro, Portugal. The overview of the research methodology is exhibited in

FIGURE 1. Input data such as approaching (Q_{in}), conflicting (Q_{conf}) and exiting (Q_{out}) traffic volumes, and queue length were collected by video cameras installed at the studied locations. Concurrently, a sound level meter was installed at the approach area of roundabouts to measure the equivalent noise sound level. On-road measurements of LDV include PEMS components for volumetric fractions of CO_2 and NO_X, and an OBD interface for vehicle activity and engine data. The relationship between congestion level of roundabouts and occurrence of each speed profile was established using discrete choice models; then, the emissions, noise and V/C ratio in SL, CTL and ML roundabouts were compared.

3.1. Study Design

FIGURE 2 depicts the aerial view of the data collection sites. Three roundabouts located on the N-235 (SL) and N-109 (CTL and ML) national roads exhibiting high traffic volumes were sought out for this study. The studied locations are in suburban environments and provide the main access to the city of Aveiro from North, South and East directions; so, the congestion and traffic related emissions and noise can constitute a specific problem in the city access.

The through movement from the East to West approach in the SL, and South to North approach in both CTL and ML layouts were examined because of high traffic volumes compared with other movements. The main approach of the ML is a two-lane located 120 m from the yield lane. Although all sites are in flat areas, CTL has an uphill road section (slope > 3%) upstream the roundabout (South-North). The posted speed limit in both CTL and ML is 50 km/h, while in SL is 60 km/h. The most relevant geometric and operational parameters of researched roundabouts are presented in Error! Reference source not found..

3.2. Field Measurements

3.2.1. On-road emissions

The measured instantaneous engine activity and speed profiles were derived from experimental data on vehicle dynamics using one LDDV complying with Euro VI emission standard and equipped with a GPS Travel Recorder (accuracy □ 5 meters) and OBD-II ELM327 Bluetooth. The testing vehicle has the following characteristics: *i*) year – 2017; *ii*) mileage – 44,000 km; *iii*) engine size – 1.2L; *iv*) transmission type – 5-speed manual gearbox; and *v*) gross vehicle weight – 1,700 kg. This LDV can be considered a point of reference for the car segment in Europe **(ICCT., 2018).**

The 3DATX ParSYNC integrated PEMS **(3DATX, 2018)** was used to perform on-road emissions tests. The device uses a single unheated sample line, which directs the sample flow through a chiller to remove water vapor before entering the unit. This lightweight PEMS measures both CO_2 (in volume fraction with a range of 0 – 20%), and NO/NO_2 (with a range of 0 – 5,000 ppm) at a frequency of 1 Hz using a replaceable GasMOD™ Sensor Cartridges for both cases. Prior study has shown the effectiveness of integrated PEMS as a tool for collecting emission data from LDV **(Leland and Stanard, 2018; Yuan et al., 2019b)**.

To ensure the accuracy of PEMS measurements, routine calibrations of pollutant analyzers (controlling for zero and span drift once per trip) were conducted using the UN 1956 gas mixture. Emissions were measured only in hot conditions, after a 30-min preconditioning period needed to let PEMS reach all the set-points.

The parSYNC does not include provision for exhaust flow measurement as it does not have an exhaust flow meter or an internal OBD reader. Thus, a Bluetooth OBD-II produced by ELM Electronics, was connected to the car's OBD socket, to collect with 1 Hz frequency the following parameters: OBD speed, mass air flow (MAF), fuel flow rate (FFR), revolutions per minute (RPM), manifold absolute pressure (MAP), intake air temperature (IAT), engine load, air-fuel ratio (A/F), barometric pressure and engine volumetric efficiency. The QSTARZ GPS Travel Recorder continuously logged vehicle position and elevation.

A temperature/pressure sensor monitored ambient temperature and humidity within each PEMS trip. Before each set of measurements, wind speed, temperature, and humidity were controlled to assure similar climate conditions among the layouts.

Monitoring campaigns were conducted during three weeks between June and July 2019 on weekdays. To account the variability of traffic operations, test sessions include several

time slots from 7:00 AM to 10:00 PM. Six male and female drivers (ages 25-39) drove the test vehicles by alternating in one-hour sessions. All test drivers respected the national law concerning the roundabout driving in ML, i.e., they entered from the left approaching lane, entered on the inner circulating lane and they only moved to the outer lane once passed the exit before the intended destination.

Prior to on-road emissions tests, the minimum number of repeat dynamometer tests on each speed profile was computed based on the standard deviation of the route-specific travel time and a tolerable error **(Fries et al., 2017)**. A total of 200 travel runs for each through movement were performed for this study (approximately 140 km of road coverage over the course of 5 hours). The above series of measurements were sufficient to enable the estimation of a 95% confidence interval **(Fries et al., 2017)**. The ranges of ambient temperatures for the studied locations were 18-21ºC, 18-22ºC and 19-22ºC in SL, CTL and ML, respectively. For humidity, the intervals were 60-85%, 75-90% and 60-80% in SL, CTL and ML, respectively. All driving sessions took place in dry and windless (< 5 $m.s^{-1}$) weather.

To isolate the effect of the roundabout layout, a fixed distance across roundabout was used to compute the complete second-by-second dynamics for a given speed profile. Thus, exhaust emissions were measured over a roundabout influence area (RIA) of 680 m, consisting of 350 m upstream the yield line.

3.2.2. Traffic volumes and noise

Entry, exit and conflicting traffic volumes, queue length, and number of vehicle stops were gathered from videotapes installed at the locations exhibited in

FIGURE 2. The first camera captured all vehicle paths through the roundabouts while the second camera recorded the queue length and idle time at the selected approaches. Then, by observing the video recordings, Q_{in}, Q_{conf} and Q_{out} were obtained for every 15 min as well as the proportion of drivers that experienced SPI, SPII and SPIII. Video recordings were collected at the same time of PEMS measurements to ensure accordance between processed traffic volumes and their impact on the registered exhaust emissions.

Concurrently, noise data were collected using a sound level meter (SLM) RION-NL-52 (Class 1 instrument). Before each measurement, the instrument was gauged using a sound calibrator RION -NC-74, with a reference signal of 94 dB at 1,000 Hz. To avoid ground reflection effects, in each location sound level meter was mounted on a tripod at 1.5 m from the ground. The distance between the sound level meter and road axis for SL, CTL and ML was 1.9 m, 1.9 m, and 1.7 m, respectively. The setup of the SLM was as follows: *i*) weighting curve A; *ii*) time constant (*F*ast) of 125 ms; and *iii*) recording of sound level pressure (*L*p) values each 100 ms.

More than 27 hours of video and noise data were collected from three roundabouts (□ 9 hours at each location), which corresponded to 106 data slots of 15-min (□ 35 data sets at each location).

3.3. Data processing and Quality Assurance

Data processing and quality assurance centered on the following steps **(Delavarrafiee and Frey, 2018; Sandhu and Frey, 2013; Yuan et al., 2019b)**: *i*) to align time of all signals recorded by all the equipment (PEMS, OBD and GNSS data); *ii*) to check data screening to remove data errors; *iii*) to estimate vehicle speed in front of the sound level meter based on hourly traffic volumes.

Time alignments were performed before calculations that depend on jointly measured data. For LDV, the recommended pairs for synchronizing OBD and PEMS data are engine speed (RPM) and NOx concentrations **(Sandhu and Frey, 2013)**. Synchronization was first evaluated by selecting the time differences that maximized the Pearson Correlation Coefficient (PCC) and followed by visualization for final confirmation. Error! Reference source not found. depicts time series plots before and after synchronization for each roundabout layout. The adjustment of RPM axis that achieved the most proper synchronization between x-axis and y-axis was +10, +6 and +9 seconds at SL, CTL and ML, respectively. The NOx-RPM produced PCC peak values between 0.34 and 0.60, which are considered to represent a well-synchronized pair according to the existing literature**(Sandhu and Frey, 2013)**.

Quality assurance screening was used to correct and eliminate erroneous data from field measurements. Typical errors include OBD data that remained constant at least 3 or more seconds, indicating that the data were no longer being updated. There are variables such as RPM, MAF, FFR and OBD speed that change with high frequency and to which CO_2 and NOx mass emissions are sensitive, making the use of linear interpolation, for instance, to obtain missing values not recommended. Although some missing values were found in raw data, the analyzed data within RIA did not present any missing value.

Negative NO and NO_2 values from PEMS were also recorded during measurements, meaning that concentration was low and below the instrument detection limit. For these cases (<0.1% of the analyzed data within RIA), negative concentrations were set to zero.

Strange events such as emergency vehicles passing, drivers honking, bells sound or pedestrian voice were detected during noise measurements. Such sporadic events are not related to normal road traffic conditions, and they cause an increase in equivalent continuous sound pressure level (L_{eq}). Therefore, the research team noted the exact

moment and type of strange events and further removed them from the raw data given by the SLM, which was set to record the sound pressure level (L_p) each 100 ms. The resulting L_p values were deleted and L_{eq} computed using the obtained filtered noise data through its relationship with L_p. In this research, strange events accounted for 0.9%, 0.8% and 0.1% of raw noise data recorded in the SL, CTL and ML, respectively.

GPS speed data in front of the SLM were associated to a 1-h slot of traffic volumes that correspond to four sequential 15-min slots. After that, a relationship between speed and $Q_{in} + Q_{conf}$ was established for each roundabout layout using a power regression analysis. It must be stressed that no data were available for all vehicles driving around roundabouts so that speed needs to be estimated for other operational conditions in order to validate the noise model, as described in **Section 3.4.4**.

3.4. Data analysis

The measured speed profiles at all roundabouts were extracted and separated for comparison to ensure consistency in the assessment of trip-specific characteristics **(Yazdani Boroujeni and Frey, 2014)**. To obtain a fair comparison among layouts, both traffic and climate conditions did not change significantly during monitoring campaigns.

3.4.1. Driving style

Driving style was characterized based on the following parameters: *i*) speeding; *ii*) relative positive acceleration (RPA); *iii*) maximum acceleration and deceleration; and *iv*) vehicular jerk.

All roundabout trips can be assigned to one of three driving styles: calm, normal severe and aggressive. These styles are based on “speeding” that is defined as “traveling at least

11% over the speed limit for more than 10 seconds" **(Gallus et al., 2017)**. Because RIA is short, speeding was both considered as the percentage of time traveling above the speed limit (v_{max}) and at least 11% over the speed limit ($1.11 \times v_{max}$).

RPA measures acceleration values during high power demand (e.g., high speed) since high accelerations associated with high torque not always demand high power**(Ericsson, 2001; Tutuianu et al., 2015)**. RPA is recognized to be a good measure of driving performance and driving behavior style, as reported in prior studies on RDE **(Fernandes et al., 2019; Gallus et al., 2017; Gallus et al., 2016)**.

RPA is computed using positive acceleration from each run, as denoted by Equations 1 and **2 (Gallus et al., 2017)**:

$$a_i = \frac{v_{i+1} - v_{i-1}}{2 \times 3.6} \ , \tag{1}$$

where:

a_i – acceleration in the second of travel i ($m.s^{-2}$)

v_{i+1} – vehicle instantaneous in the second of travel i +1 ($km.h^{-1}$);

v_{i-1} – vehicle instantaneous in the second of travel i -1 ($km.h^{-1}$).

$$RPA = \frac{\sum_i \frac{v_i}{3.6} \times a_i^+}{d} \ , \tag{2}$$

where:

RPA – Relative positive acceleration ($m.s^{-2}$);

a_i^+ – Positive values of the acceleration for the second of travel i ($m.s^{-2}$);

d – Total distance of the trip (m).

The following RPA thresholds by road type in accordance with the Worldwide Harmonized Light duty driving Test Cycle (WLTC) were used **(Gallus et al., 2017)**: 0.12 $m.s^{-2}$ (urban); and 0.14 $m.s^{-2}$ (rural).

Driving style was also characterized using maximum acceleration and deceleration, and vehicular jerk (change rate of vehicle acceleration with respect to time, i.e., first derivate of acceleration/deceleration, denoted as j) that can be applied to suburban areas, as follows: maximum acceleration of 2.16 $m.s^{-2}$ **(Choi and Kim, 2017)**; maximum deceleration of 3.4 $m.s^{-2}$ **(Deligianni et al., 2017)** and vehicular jerk of 0.9 $m.s^{-3}$ **(Liu, 2015)**. For the purpose of the analysis, the percentage of time spent above thresholds was computed by speed profile and roundabout layout.

3.4.2. Predictive Choice Models

This paper used a process of discrete choice of speed profiles (SPI, SPII **and SPIII) to** predict the relative occurrence of each speed profile based on current congestion levels. It is based on stochastic processes, in which the decision maker makes a choice that optimizes the utility function, in this case, the prediction of probability of a driver performing a speed profile. A multinomial logistic regression model (MLRM) was applied to predict the probability of occurrence of each speed profile at SL, CTL and ML based on the collected data samples **(Correia and Silva, 2010)**. The utility function is defined in Equation 3.

$$U_{i,\mathrm{n}} = V_{i,\mathrm{n}} + \varepsilon_{i,\mathrm{n}}, \tag{3}$$

where

$V_{\mathrm{i,n}}$ – Systematic part of the utility function that gives the prediction of the probability of the driver *n* performing speed profile $i \in I,\ I = \{\mathrm{I,II,III}\}$;

$\varepsilon_{i,\mathrm{n}}$ – Error between the systematic part and the true utility of driver *n* performing speed profile *i*.

Assuming the error follows a logistic distribution and by algebraic manipulation, the prediction of probability of occurrence of SPI, SPII and SPIII is given by Equations 4, 5 and 6, respectively:

$$P_{SPI} = \frac{1}{1 + e^{\beta_{2,0} + (\beta_{2,1} \times [Q_{\mathrm{in}} + Q_{\mathrm{conf}}])} + e^{\beta_{3,0} + (\beta_{3,1} \times [Q_{\mathrm{in}} + Q_{\mathrm{conf}}])}}, \tag{4}$$

$$P_{SPII} = \frac{e^{\beta_{2,0} + (\beta_{2,1} \times [Q_{\mathrm{in}} + Q_{\mathrm{conf}}])}}{1 + e^{\beta_{2,0} + (\beta_{2,1} \times [Q_{\mathrm{in}} + Q_{\mathrm{conf}}])} + e^{\beta_{3,0} + (\beta_{3,1} \times [Q_{\mathrm{in}} + Q_{\mathrm{conf}}])}},$$

(5)

$$S_{SPIII} = \frac{e^{\beta_{3,0} + (\beta_{3,1} \times Q_{\mathrm{in}})}}{1 + e^{\beta_{2,0} + (\beta_{2,1} \times [Q_{\mathrm{in}} + Q_{\mathrm{conf}}])} + e^{\beta_{3,0} + (\beta_{3,1} \times [Q_{\mathrm{in}} + Q_{\mathrm{conf}}])}}, \tag{6}$$

where:

P_{SPI} – Prediction of the probability of occurrence of vehicles experiencing SPI;

$\beta_{2,0}$ – Intercept for outcome of SPII;

$\beta_{2,1}$ – Coefficient for outcome of SPII;

Q_{in} – Number of approaching vehicles (vehicles per hour – vph);

Q_{conf} – Number of conflicting vehicles (vph);

$\beta_{3,0}$ – Intercept for outcome of SPIII;

$\beta_{3,1}$ – Coefficient for outcome of SPIII;

P_{SPII} – Prediction of the probability of occurrence of vehicles experiencing SPII;

P_{SPIII} – Prediction of the probability of occurrence of vehicles experiencing SPIII.

The β parameters were estimated from the collected data sample and ultimately optimize the utility function, i.e., the prediction of the probability of driver n having the outcome of performing speed profile i over the reference SPI for each roundabout layout under existing traffic conditions. The intercept parameter relates with the logarithmic odd of speed profile i occurring when $Q_{in} + Q_{conf}$ tends to 0; therefore, the negative intercepts obtained translate into small odds of SPII and SPIII occurring under low congestion levels as observed. The coefficient parameter indicates how SPII and SPIII are expected to develop as $Q_{in} + Q_{conf}$ increases. Since coefficient parameters present positive values, SPII and SPIII are expected to have higher prediction of the probability of occurrence as congestion increases.

A leave-one-out cross validation (LOOCV) method was applied to test if the estimated β coefficients are able to precisely characterize the collected data sample. LOOCV is a special case of the k-fold cross-validation where the number of groups – k is equal to the of number of testing samples – n. This method was chosen since it provides an approximately unbiased exhaustive cross validation compared to the stratified holdout and k-fold cross validation approaches **(Kanevski et al., 2009).**

3.4.3. Mass Emission Rates

The method described by the Regulatory Information 40 CFR 86.144 for exhaust emissions was used to compute pollutant mass at each second **(EPA, 2018)**. Based on exhaust flow rate and exhaust gas concentrations, emission rates of NO, NO_2 and CO_2 (mass per time unit) were estimated. For the purpose of this paper, the sum of concentration signals for NO and NO_2 corresponds to the NOx concentration **(Sandhu and Frey, 2013)**. If neither MAF nor MFF are reported by electronic control unit (ECU), then MAF can be inferred from RPM, MAP, and IAT using the speed density method given in Equation 7 **(Sandhu and Frey, 2013)**:

$$M_{\text{air}} = MW_{\text{air}} \frac{\left(P_{\text{MAP}} - \frac{P_B}{C_{\text{engine}}}\right) \times V_{\text{engine}} \left(\frac{S_{\text{engine}}}{120}\right)}{R\left(T_{\text{intake}} + 273.15\right)} \eta_{\text{engine}}, \quad (7)$$

where:

M_{air} – Mass air flow rate ($g.s^{-1}$);

MW_{air} – Molecular weight of the air (28.9 $g.mol^{-1}$);

P_{MAP} – MAP (kPa);

P_B – Barometric pressure (kPa);

C_{engine} – Engine compression ratio (dimensionless);

V_{engine} – Engine size (L);

S_{engine} – Engine speed in revolutions per minute (rpm);

η_{engine} – Engine volumetric efficiency (dimensionless);

R – Universal gas constant (8.314 J/mol/K);

T_{intake} – IAT (ºC).

Otherwise, it is possible to correlate the fuel mass flow rate to the air mass flow rate by means of the A/F (given by OBD) using Equation 8 **(Grimaldi and Millo, 2015)**:

$$A/F = \frac{\dot{m}_{air}}{\dot{m}_{fuel}} \ , \tag{8}$$

where:

$\dot{m}_{air}$ – Mass air flow rate (g.s^{-1});

$\dot{m}_{fuel}$ – Fuel mass flow rate (g.s^{-1}).

The exhaust flow rate is therefore the sum of the air flow and flue flow rates. CO_2 and NO_X mass emission rates were estimated **(EPA, 2018)**, respectively, as:

$$m_{CO_2} = \dot{V}_{exhaust} \ \rho_{CO_2} X_{CO_2} \ , \tag{9}$$

$$m_{NO_X} = \dot{V}_{ex} \ \rho_{NO_X} X_{NO_X} \frac{1}{1-0.0047\left(H-75\right)} \ , \tag{10}$$

where:

$\dot{V}_{exhaust}$ – Exhaust volumetric flow rate (corrected to standard conditions) (m^3.s^{-1});

ρ_{CO2} – Density of CO_2 at the standard conditions (1.830 kg.m^{-3});

X_{CO2} – Volume fraction of CO_2 measured by PEMS (%).

ρ_{NOX}– Density of NO_X at the standard conditions (1.913 kg.m^{-3});

X_{NOX} – Volume fraction of NO_X measured by PEMS (ppm);

H – Humidity (%).

Next, pollutant emissions per vehicle for the three speed profiles were aggregated to evaluate the overall impact of a change in the average path through the SL, CTL and ML. The estimation of hourly emissions generated by vehicles entering a generic roundabout is expressed as follows:

$$E_j = Q_{in}\left(E_{I,j} \times P_I + E_{II,j} \times P_{II} + E_{III,j} \times P_{III}\right), \quad (11)$$

where

E_j – Predicted emissions of specie $j \in J$, J = (CO_2, NO_X) (g);

$E_{I,j}$ – Predicted emissions per vehicle associated with SPI for specie j (g);

P_I – Prediction of the probability of occurrence of vehicles experiencing SPI;

$E_{II,j}$ – Predicted emissions per vehicle associated with SPII for specie j (g);

P_{II} – Prediction of the probability of occurrence of vehicles experiencing SPII;

$E_{III,j}$ – Predicted emissions per vehicle associated with SPIII for specie j (g);

P_{III} – Prediction of the probability of occurrence of vehicles experiencing SPIII.

3.4.4. Traffic Noise

Quartieri et al. (2010) model was validated against noise measurements conducted with the sound level meter. This semi-dynamical model uses traffic volumes (by lane) and average vehicle speed to estimate the equivalent continuous A-weighted sound level for a specific lane (hourly basis), as follows:

$$L_{eq}^{1h} = 10\log\left[V_{\text{LDV}} + n_{\text{V}} \times V_{\text{HDV}}\right] + L_{w,i} - 20\log(d) - 46.563\,, \tag{12}$$

where:

V_{LDV} – Hourly LDV volumes (vph);

n_{V} – Equivalent acoustic factor that represents the number of LDV that produce the same sound energy of one HDV;

V_{HDV} – Hourly HDV volumes (vph);

$L_{w,i}$ – Source power level of LDV (dBA);

d – Distance between the observation point and the road axis (m).

The equivalent acoustic factor depends on the vehicle speed and driving state (cruising/deceleration and deceleration). More details about the calculation can be found in **(Quartieri et al., 2010)**. Thus, the source power level for $L_{w,i}$ (LDV) is obtained using according to Equation 13 **(Lelong J., 1999)**:

$$L_{w,i} = \alpha_L + \beta_L \log(v) \ , \tag{13}$$

where:

v – Average vehicle speed (km.h^{-1});

α_L = 53.6 ± 0.3 dBA and β_L = 26.8 ± 0.2 dBA, according to **(Quartieri et al., 2010)**.

To account for the effect of all approaching and exiting lanes, the total hourly equivalent continuous A-weighted sound level is given by Equation 14:

$$L_{eq,tot}^{1h} = 10 \log \left(\sum_{i=1}^{t} 10^{\frac{L_{eq,i}^{1h}}{10}} \right) , \tag{14}$$

where:

$L_{eq,tot}^{1h}$ – Total hourly equivalent continuous A-weighted sound level (dBA)

t – Number of the approaching and exiting lanes (CTL/SL – 1+1; ML – 2+2);

$L_{eq,i}^{1h}$ – Hourly equivalent continuous A-weighted sound level for a lane i (dBA).

To assess the goodness of fit, a bisector plot was built to compare measured and estimated noise, as suggested by **Guarnaccia et al. (2018)**. Thus, measured data points were plotted against the estimated ones, and then the bisector was shifted up and down by 3 dBA. This range was used as a guide to the eye because it corresponds to the doubling or halving of the squared sound pressure. Moreover, the absolute percentage errors (APE) between the

estimated L_{Aeq} and the recorded ones were computed for each measurement. Finally, the Mean Absolute Percentage Error (MAPE) for each roundabout was obtained as the average of the APEs.

3.4.5. Volume-to-Capacity

The methodology in the Highway Capacity Manual (HCM) was followed to characterize the V/C ratio at the studied locations. Movement demand flows for the measured 15-min period were first converted to hourly values, then the flow rates were adjusted according to the Equation 15 **(HCM, 2016)**:

$$V_{i,pce} = \frac{V_i}{1 + P_T\left(E_T - 1\right)}\ , \tag{15}$$

where:

$V_{i,pce}$ – Demand flow for movement *i* (passenger car units per hour – $pcu.h^{-1}$);

V_i – Demand flow for movement *i* ($pcu.h^{-1}$);

P_T – Proportion of demand volume consisting of heavy vehicles (dimensionless);

E_T – Passenger car equivalent for heavy vehicles [2, as suggested in **(Giuffrè et al., 2019)**].

Since the capacity of a roundabout approach is influenced by local driving habits, a generalized Siegloch model in the form of Equation 16 was used **(HCM, 2016)**:

$$C_{e,pce} = \frac{3,600}{t_f} \times e^{\left(-\left(\frac{t_c - 0.5 \times t_f}{3,600}\right)\right) V_{c,pce}} \times f_{\text{ped}} \ , \quad (16)$$

where:

$C_{e,pce}$ – Capacity of the entry leg (pcu.h^{-1});

$V_{e,pce}$ – Conflicting flow (pcu.h^{-1});

t_f – Critical headway (s);

t_c – follow-up headway (s);

f_{ped} – Pedestrian impedance to vehicles (dimensionless).

The full range of t_c and t_f for local conditions were 3.82-4.27 s and 2.72-3.10 s, respectively **(Giuffrè et al., 2016; Vasconcelos AL et al., 2013)**. Because pedestrian activity was small (< 10 pedestrians per hour), the f_{ped} was set 1. Finally, the V/C of the movement is the ratio between $V_{i,pce}$ and $C_{e,pce}$ computed by Equation 15 and Equation 16, respectively.

4. Results

This section first presents and discusses the main results from field measurements (**Section 4.1**) followed by speed profile predictive models (**Section 4.2**) and noise model evaluation (**Section 4.3**). Finally, CO_2 and NOx emissions, noise and V/C ratio of each layout are compared.

4.1. Traffic performance and emissions

TABLE 2 lists the main traffic performance and emission results of each roundabout layout and speed profile. Results indicated that SL had on average lower travel (15% and 13%) and idle (40% and 60%) times, and CO_2 per kilometer (20% and 5%) compared to CTL and ML, respectively. However, drivers in the SL emitted 7% more NO_X per kilometer than in the ML. This may be due to sharp acceleration episodes (3% more RPA events in SL than in ML), which in turn have an impact on NO_X. The coefficient of variability of NO_X was 0.43, 0.38 and 0.34 for SL, CTL and ML, respectively. Another reason for these results is that the acceleration rate of vehicles tends to increase as Q_{conf} decreases **(Coelho et al., 2006)**. This is the case of SL where conflicting traffic is low (Q_{conf} < 150 vph) in several periods of the day. Although CTL achieved similar performance levels to ML, it presented the highest emission levels. The analysis showed a different trend by speed profile among layouts. For SPI, vehicles at the ML produced less pollutant emissions (CO_2 –21%; NO_X – 48%) than vehicles in the CTL. This layout also had 21% lower NO_X compared with SL. As expected, vehicles spent lower travel times crossing SL, given an equal RIA, which is explained by high approaching speeds at this layout (see Error! Reference source not found. for those details).

CO_2 and NO_X emission rates, acceleration and vehicular jerk distributions in each 20 m segment length are exhibited in **Error! Reference source not found.**. The values in the graphs represent the average values of all runs performed per roundabout. Downstream was the emission hotpot location regardless of the layout, but the impacts in this segment were more noticeable in NO_X compared to CO_2. For instance, vehicles generated in the first 150 m (22% of RIA) after exiting the roundabout 29%, 30%, 41% of CO_2, and 32%, 35%, 51% of NOx, respectively for SL, CTL, and ML. Emission rates at downstream

were higher at CTL compared to other layouts. This resulted from the difference between circulating and cruise speeds, which was high in CTL, as presented in Error! Reference source not found.**.** Acceleration was found to be notably high in both circulating and downstream areas, but some differences were identified among layouts. In fact, the average acceleration was 0.50 $m.s^{-2}$ at the downstream of CTL, which was 65% and 45% higher than the values observed at SL and ML, respectively. Circulating areas were the main affected by vehicular jerk (an indicator of driving volatility), especially in SL (2.5 times higher than the SL average) and CTL (9 times higher than the CTL average). These findings are relevant since this kinetic variable is widely associated with aggressive driving and hard braking maneuvers. Since vehicles experienced fast gear changes, some jerk peaks were also observed at upstream of roundabouts.

To assess driving behavior, Error! Reference source not found. lists the percentage of time spent above thresholds of speeding, acceleration-deceleration and vehicular jerk, as well as the percentage of trips above the RPA thresholds for urban and rural areas. The weight of extreme acceleration and deceleration and a_i^+ at SL was, on average, lower than the other roundabout layouts. For instance, extreme acceleration and deceleration represented together 1.2%, 1.6% and 5.7% of SL, CTL and ML total trip time, respectively. Curiously, SL was associated with higher RPA (see **Error! Reference source not found.**), but the percentage of the time spent in accelerations higher than 0.1 $m.s^{-2}$ and the percentage of trips above the urban and rural literature RPA thresholds were generally low when compared to the other layouts. This result is pertinent since SL had the lowest travel times. Although speeding did not vary among layouts, on average, drivers exceeded at least 10% over the roundabout-specific speed limit. The results for

jerk confirmed a greater percentage of jerk values higher than 0.9 $m.s^{-3}$ at ML, especially at SPIII. This fact indicates higher volatility than SL and CTL.

4.2. Speed profiles predictive models

Three MLRM were completed, one per each roundabout layout. The parameters of each regression were calibrated using SPSS software (**Error! Reference source not found.**). The data sample covered **4,720, 4,201 and 8,721** observations taken at SL, CTL and ML, respectively. These samples were gathered in a database with three fields: roundabout layout (SL, CTL and ML), speed profile (SPI, SPII, and SPIII) and Q_{total} (Q_{in} + Q_{conf}, in 15-min period). The estimated β parameters obtained are statistically significant (p-value < 0.10, p-value < 0.05, and p-value < 0.01, for significance levels of 10%, 5%, and 1%, respectively), meaning that the predictions of the probability of occurrence of SPII and SPIII fit well with field data sample. The LOOCV method was applied, and a total of 26 MLRMs were developed (k = 8 for SL, k = 8 for CTL, and k = 10 for ML) to test the performance of the general models (3 MLRMs, 1 for each roundabout layout). Supplementary data contains detailed information about the models obtained to develop the LOOCV approach by roundabout. To assess the goodness of fit, the mean absolute error (MAE) and the root-mean-square error (RMSE) were used. Error! Reference source not found. reveals that the developed models are able to predict the probability of occurrence accurately, i.e., the MAE range and RMSE range amongst the testing models were 2%-11% and 2%-7% at SL, 1%-9% and 1%-6% at CTL, and 8%-16% and 5%-10% at ML. Furthermore, the general models showed identical percentages of occurrence of each speed profile between observed and predicted data.

Intuitively, the probability of the driver to enter the roundabout without **stopping (P_{SPI})** decreases as the traffic flow increases, as shown in Error! Reference source not found.. It

can be observed that more than 50% of vehicles enter the SL without stopping for Q_{total} lower than 1,800 vph, while at CTL and ML this occurred for values lower than 1,200 and 1,000 vph, respectively. It must be noted that SL has lower conflicting traffic (9% of Q_{total}) compared to the other layouts (>13% of Q_{total}) hence a cause to the obtained results. The analysis of the collected data at each roundabout layout indicates that different combinations of Q_{in} + Q_{conf}, with the same Q_{total}, generally result in the same distribution of the probability of occurrence of each speed profile. No specific pattern was identified for higher/lower Q_{in} or Q_{conf} resultant from the same Q_{total}. Such a fact implies that Q_{in} or Q_{conf} should be explored jointly. Additionally, when considering different Q_{total}, and either Q_{in} or Q_{conf} being constant while the other increases, SPII and SPIII obtain higher probabilities of occurrence, as can also be perceived subliminally. For traffic flows higher than 1,800 vph, approximately 30% of vehicles at SL and CTL, and 70% at ML, will face multiple stops. This substantial difference observed at ML was due to the fact that the probability was calculated considering the left lane approach and high Q_{conf} (>350 vph) was observed.

4.3. Traffic noise evaluation

The field measurements showed higher values of L_{Aeq} at SL for two reasons: 1) high approaching speeds; and 2) high percentage of HDV and motorcycles (10% compared to 5% and 7% for CTL and ML, respectively). Quartieri et al. model was applied to the data sample, and estimated L_{eq} presented goodness of fit compared with the recorded ones, as shown in Error! Reference source not found.. The APE between the L_{Aeq} estimated and observed ranged from 0.1% to 5.7% (depending on the roundabout layout) while the resulting MAPE was 1.7%, 2.0% and 2.8% at the SL, CTL and ML, respectively. The maximum difference obtained between estimated and recorded L_{Aeq} was around 3.5 dBA. Since this model does not consider the acceleration of the vehicles, it tends to

underestimate L_{Aeq} under congested traffic conditions. This explained the differences obtained in the ML, where idle time was higher than in the other layouts, as presented in **Error! Reference source not found.**.

4.4. Scenarios

This section uses discrete predictive models, trajectories associated to SPI, SPII and SPIII to compare pollutant emissions, noise and V/C of each layout. Thus, five traffic demand scenarios were explored, as follows:

- S1: Q_{total} = 400 vph and Q_{out} = 350 vph;
- S2: Q_{total} = 800 vph and Q_{out} = 700 vph;
- S3: Q_{total} = 1,200 vph and Q_{out} = 1,000 vph;
- S4: Q_{total} = 1,600 vph and Q_{out} = 1,350 vph;
- S5: Q_{total} = 2,000 vph and Q_{out} = 1,700 vph.

S1 and S2 are typical from off-peak hour conditions, while S3 to S5 can represent peak-hour periods. The comparison of hourly predicted pollutant emissions per vehicle, noise and V/C ratio for each roundabout layout is displayed in

FIGURE 7. Findings indicated that CTL generated the highest amount of pollutant emissions per vehicle, regardless of the testing scenario. On average, vehicles produced 32% and 21% more CO_2 than vehicles at SL and ML, respectively. The results for NO_X were even worse (65% and 75% higher than SL and ML, respectively). Although SL showed as the best option in terms of CO_2 (mostly due to lower travel times), it generated more NO_X than ML under low and moderate traffic demands (S1-S4**).** This was possible

due to accelerations at high speeds to which NOx emissions in LDDV are sensitive. The results for noise dictated different outcomes: SL was expected to achieve a high L_{Aeq} (> 67 dBA) under low and moderate traffic demands (S1-S3) because vehicles in the SL experienced higher approaching speeds than vehicles in CTL and ML did. It was also found that CTL presented higher L_{Aeq} than ML in almost all scenarios. This may occur due to the high percentage of motorcycles. Interestingly, the studied SL and CTL approach reached saturation at S3, while ML saturated at higher values (S4). This explains the high L_{Aeq} values obtained in ML at this latter scenario, i.e., vehicles drove at moderated speeds with the same traffic volume (at CTL the speed values are near 0). The graphs in

FIGURE 7 also showed differences between off-peak (S1-S2) and peak hour (S3-S5) conditions among roundabout layouts. In this case, CO_2 emissions increased up to 7%, 9% and 15% in SL, CTL and ML, respectively, while NO_X per vehicle during oversaturation periods rose between 5% and 20% in SL and ML.

The above results confirmed that a given SL with specific operational (high through traffic demand and unbalanced traffic flows between main roads and minor roads) and design (higher entry speeds) features could be adopted in suburban environments instead of CTL or ML. Speed profiles distribution influences the amount of CO_2 and NOx emissions emitted by vehicles, while entry and exit speeds can result in different noise levels. This fact implies that different traffic operations and speed limits could result in different performance in the same layout. For example, a single-lane roundabout exhibiting lower traffic volumes and entry speeds, and higher conflicting traffic could possibly be more comparable to a compact two-lane roundabout. Accordingly, there is a

need for comparison under similar traffic conditions both in terms of demand and fleet compositions.

5. CONCLUSIONS

This paper explored the impact of SL, CTL and ML roundabouts installed in suburban environments on traffic performance, pollutant emissions, noise and capacity. The proposed methodology was grounded in empirical data of vehicle activity and emissions, traffic volumes and noise to assess traffic performance, CO_2 and NO_X, L_{Aeq} and V/C ratios. This paper also developed predictive discrete choice models between the probability of speed profiles and site-specific operational parameters.

Field measurements indicated that SL generated lower travel time (13-15%) and CO_2 emissions per unit distance (5% -20%) compared to ML and CTL roundabouts. However, it yielded higher RPA (10% higher on average) and NO_X emissions per unit distance than the ML roundabout. The implementation of predictive discrete choice models in five combinations of approaching, conflicting and exiting traffic volumes pointed out differences among layouts. SL yielded the lowest CO_2 per vehicle, assuming an equal RIA since vehicles spent less time driving towards roundabout together with low conflicting traffic. However, its implementation can result in higher L_{Aeq} at low traffic volumes because vehicles drove at higher speeds in the approach compared to the other layouts.

This research has two main scientific contributions: first, it addressed the impacts of a specific roundabout layout on pollutant emissions and noise using field measurements, thus reflecting site-specific driving behavior and traffic conditions. There is potential to embed this methodology in current simulation tools to predict emissions or noise of road traffic for use in traffic, emissions and air quality strategies. Second, it introduced a

framework that integrated operational and environmental parameters through the identification of the occurrence of typical speed profiles. This was done by using discrete choice models that were capable of identifying the three speed profiles that account for location-specific needs and variability characteristics in the measured data.

As result of attributes of these roundabouts (high approaching speeds, negligible pedestrian and cyclist activity), this research can provide relevant information pertaining pollutant and noise emissions comparison between roundabouts and other traffic control treatments such as traffic lights and stop-controlled intersections. This could support traffic planners, local authorities and other practitioners to prevent congestion at roundabouts and resulting negative impacts on global warming (CO_2) and air pollution (NO_X and noise).

Although results cannot be generalized to all sites, this empirical methodology is suitable in quantifying the performance of other roundabout layouts, using the following steps: 1) to gather entry and conflicting hourly volumes allows the use of discrete choice models to predict the probability of vehicles performing SPI, SPII and SPIII; 2) to assign a vehicle trajectory to a speed profile (SPI, SPII and SPIII), and vehicle type; 3) to compute emissions by multiplying the entry traffic flow by the sum of the product of the percentage of occurrence of each speed profile with the associated emission factor; 4) to collect exit and entry traffic volumes and speed allows to estimate noise levels; and 5) to estimate V/C ratio based on collected traffic data and local driving habits.

However, there are some limitations that must be outlined: 1) only one vehicle type was used in the experimental analysis; 2) predictive discrete choice models were based on site-specific entry and conflicting traffic volumes, which are only replicable in other roundabouts with similar traffic conditions; otherwise, a new MLRM should be developed and applied; and 3) noise model does not consider acceleration, which is

predominantly high under high traffic volumes and stop-and-go situations, thus underestimating the L_{Aeq}. Future work must be focused on additional real driving emissions of gasoline and hybrid passenger cars with different emission standards. The development of a noise model that considers more kinetic variables such as acceleration and jerk should also be developed. There is a need for more widespread conditions to increase the potential of developed work. Therefore, inclusion of other roundabouts with the same layout but different traffic conditions (for instance, a SL with high conflicting traffic) and different layouts (turbo-roundabouts), as well as other types of intersections (traffic lights and stop-controlled intersections) should also be explored. Further development concerning the relationship between geometric features of suburban roundabouts such as entry radius, exit radius, number of lanes and IDC on the probability of speed profiles, traffic volumes, and speed would be relevant to explore their impacts on roundabout-specific capacity, emissions and noise levels.

Declaration of interests

The authors declare that they have no known competing financial interests or personal relationships that could have appeared to influence the work reported in this paper.

ACKNOWLEDGEMENTS

The authors acknowledge the financial support of the following projects: UIDB/00481/2020 and UIDP/00481/2020 - FCT - Fundação para a Ciência e a Tecnologia; and CENTRO-01-0145-FEDER-022083 - Centro Portugal Regional Operational Programme (Centro2020), under the PORTUGAL 2020 Partnership Agreement, through the European Regional Development Fund; MobiWise (P2020 SAICTPAC/0011/2015), co-funded by COMPETE2020, Portugal2020 - Operational

Program for Competitiveness and Internationalization (POCI), European Union's ERDF (European Regional Development Fund), and FCT; DICA-VE (POCI-01-0145-FEDER-029463), funded by FEDER through COMPETE2020, and by National funds (OE), through FCT/MCTES.

6. REFERENCES

3DATX, 2018. http://www.3datx.com/, 3-dimensional data analysis (3DATX) Corporation.

Brilon, W., 2014. Roundabouts: a state of the art in Germany, Paper Presented at the Transportation Research Board 4th International Roundabout Conference, Seattle, WA, United States.

Can, A., Aumond, P., 2018. Estimation of road traffic noise emissions: The influence of speed and acceleration. *Transportation Research Part D: Transport and Environment* 58, 155-171.

Chauhan, B.P., Joshi, G.J., Parida, P., 2018. Driving cycle analysis to identify intersection influence zone for urban intersections under heterogeneous traffic condition. *Sustainable Cities and Society* 41, 180-185.

Chevallier, E., Leclercq, L., Lelong, J., Chatagnon, R., 2009. Dynamic noise modeling at roundabouts. *Applied Acoustics* 70(5), 761-770.

Choi, E., Kim, E., 2017. Critical aggressive acceleration values and models for fuel consumption when starting and driving a passenger car running on LPG. *International Journal of Sustainable Transportation* 11(6), 395-405.

Coelho, M.C., Farias, T.L., Rouphail, N.M., 2006. Effect of roundabout operations on pollutant emissions. *Transportation Research Part D: Transport and Environment* 11(5), 333-343.

Correia, G., Silva, A., 2010. Setting Speed Limits on Rural Two-Lane Highways by Modeling the Relationship between Expert Judgment and Measurable Roadside Characteristics. *Journal of Transportation Engineering* 137(3), 184-192.

Covaciu, D., Florea, D., Timar, J., 2015. Estimation of the noise level produced by road traffic in roundabouts. *Applied Acoustics* 98, 43-51.

Delavarrafiee, M., Frey, H.C., 2018. Real-world fuel use and gaseous emission rates for flex fuel vehicles operated on E85 versus gasoline. *Journal of the Air & Waste Management Association* 68(3), 235-254.

Deligianni, S.P., Quddus, M., Morris, A., Anvuur, A., Reed, S., 2017. Analyzing and Modeling Drivers' Deceleration Behavior from Normal Driving. *Transportation Research Record* 2663(1), 134-141.

EEA, 2018. Population exposure to environmental noise. European Environment Agency, Retrieved from: https://www.eea.europa.eu/data-and-maps/indicators/exposure-to-and-annoyance-by-2, Accessed date: 20 March 2019.

EEA, 2019. Small increase in EU's total greenhouse gas emissions in 2017, with transport emissions up for the fourth consecutive year European Environment Agency, Retrieved from:

https://www.eea.europa.eu/downloads/7bd65ddadd0c44cd8f45a30ba9fbe92c/1559127729/small-increase-in-eus-total-ghg.pdf, Accessed date: 20 November 2019.
EPA, 2018. Title 40 - Protection of Environment, Section 86.144-94 - Calculations; exhaust emissions., United States Environmental Protection Agency, Retrieved from: https://www.govinfo.gov/content/pkg/CFR-2012-title40-vol19/xml/CFR-2012-title40-vol19-sec86-144-94.xml, Accessed date: 7 July 2019
Ericsson, E., 2001. Independent driving pattern factors and their influence on fuel-use and exhaust emission factors. *Transportation Research Part D: Transport and Environment* 6(5), 325-345.
Estévez-Mauriz, L., Forssén, J., 2018. Dynamic traffic noise assessment tool: A comparative study between a roundabout and a signalised intersection. *Applied Acoustics* 130, 71-86.
Fernandes, P., Coelho, M., 2019. Making Compact Two-Lane Roundabouts Effective for Vulnerable Road Users: An Assessment of Transport-Related Externalities. Springer International Publishing, Cham, pp. 99-111.
Fernandes, P., Guarnaccia, C., Teixeira, J., Sousa, A., Coelho, M.C., 2017a. Multi-Criteria Assessment of Crosswalk Location on a Corridor with Roundabouts: Incorporating a Noise Related Criterion. *Transportation Research Procedia* 27, 460-467.
Fernandes, P., Macedo, E., Bahmankhah, B., Tomas, R.F., Bandeira, J.M., Coelho, M.C., 2019. Are internally observable vehicle data good predictors of vehicle emissions? *Transportation Research Part D: Transport and Environment* 77, 252-270.
Fernandes, P., Pereira, S.R., Bandeira, J.M., Vasconcelos, L., Silva, A.B., Coelho, M.C., 2016. Driving around turbo-roundabouts vs. conventional roundabouts: Are there advantages regarding pollutant emissions? *International Journal of Sustainable Transportation* 10(9), 847-860.
Fernandes, P., Rouphail, N.M., Coelho, M.C., 2017b. Turboroundabouts Along Corridors: Analysis of Operational and Environmental Impacts. *Transportation Research Record* 2627(1), 46-56.
Fernandes, P., Salamati, K., Rouphail, N.M., Coelho, M.C., 2015. Identification of emission hotspots in roundabouts corridors. *Transportation Research Part D: Transport and Environment* 37, 48-64.
Fernandes, P., Teixeira, J., Guarnaccia, C., Bandeira, J.M., Macedo, E., Coelho, M.C., 2018. The Potential of Metering Roundabouts: Influence in Transportation Externalities. *Transportation Research Record* 2672(25), 21-34.
Frey, H.C., Zhang, K., Rouphail, N.M., 2008. Fuel Use and Emissions Comparisons for Alternative Routes, Time of Day, Road Grade, and Vehicles Based on In-Use Measurements. *Environmental Science & Technology* 42(7), 2483-2489.
Fries, R., Qi, Y., Leight, S., 2017. How many times should I run the Model? Performance Measure. Specific Findings from VISSIM models in Missouri, *96th Annual Meeting of the Transportation Research Board, Washington, DC*.
Gallus, J., Kirchner, U., Vogt, R., Benter, T., 2017. Impact of driving style and road grade on gaseous exhaust emissions of passenger vehicles measured by a Portable Emission Measurement System (PEMS). *Transportation Research Part D: Transport and Environment* 52, 215-226.
Gallus, J., Kirchner, U., Vogt, R., Börensen, C., Benter, T., 2016. On-road particle number measurements using a portable emission measurement system (PEMS). *Atmospheric Environment* 124, 37-45.
Gardziejczyk, W., Motylewicz, M., 2016. Noise level in the vicinity of signalized roundabouts. *Transportation Research Part D: Transport and Environment* 46, 128-144.

Garg, N., Maji, S., 2014. A critical review of principal traffic noise models: Strategies and implications. *Environmental Impact Assessment Review* 46, 68-81.
Gastaldi, M., Meneguzzer, C., Giancristofaro, R.A., Gecchele, G., Lucia, L.D., Prati, M.V., 2017. On-road measurement of CO2 vehicle emissions under alternative forms of intersection control. *Transportation Research Procedia* 27, 476-483.
Giuffrè, O., Granà, A., Giuffrè, T., Tumminello, M.L., Acuto, F., 2019. Passenger Car Equivalents for Heavy Vehicles at Roundabouts. a Synthesis Review. *Frontiers in Built Environment* 5(80), 1-12.
Giuffrè, O., Granà, A., Tumminello, M.L., 2016. Gap-accepteance parameters for roundabouts: a systematic review. *European Transport Research Review* 8(1), 1-20.
Givargis, S., Mahmoodi, M., 2008. Converting the UK calculation of road traffic noise (CORTN) to a model capable of calculating LAeq,1h for the Tehran's roads. *Applied Acoustics* 69(11), 1108-1113.
Grimaldi, C.N., Millo, F., 2015. Internal Combustion Engine (ICE) Fundamentals, In: Wiley (Ed.), pp. 1-32.
Guarnaccia, C., 2010. Analysis of Traffic Noise in a Road Intersection Configuration. *WSEAS Transactions on Systems* 9(8), 865-874.
Guarnaccia, C., 2013. Advanced tools for traffic noise modelling and prediction. *WSEAS Transactions on Systems* 12(2), 121-130.
Guarnaccia, C., Bandeira, J., Coelho, M.C., Fernandes, P., Teixeira, J., Ioannidis, G., Quartieri, J., 2018. Statistical and semi-dynamical road traffic noise models comparison with field measurements. *AIP Conference Proceedings* 1982(1), 020039.
Hallmark, S.L., Wang, B., Mudgal, A., Isebrands, H., 2011. On-Road Evaluation of Emission Impacts of Roundabouts. *Transportation Research Record* 2265(1), 226-233.
HCM, 2016. Highway Capacity Manual, Sixth Edition: A Guide for Multimodal Mobility Analysis , Chapter 22 Roundabouts, Transportation Research Board, Washigton DC.
ICCT., 2018. European Vehicle Market Statistics Pocketbook 2018/2019 [Internet]. ICCT – The International Council on Clean Transportation, Berlin, Germany. Available from:
https://theicct.org/sites/default/files/publications/ICCT_Pocketbook_2018_Final_20190408.pdf.
Jaworski, A., Mądziel, M., Lejda, K., 2019. Creating an emission model based on portable emission measurement system for the purpose of a roundabout. *Environmental Science and Pollution Research* 26(21), 21641-21654.
Kanevski, M., Timonin, V., Pozdnukhov, A., 2009. *Machine Learning for Spatial Environmental Data: Theory, Applications, and Software*. CRC Press.
Kephalopoulos, S., Paviotti, M., Anfosso-Lédée, F., Van Maercke, D., Shilton, S., Jones, N., 2014. Advances in the development of common noise assessment methods in Europe: The CNOSSOS-EU framework for strategic environmental noise mapping. *Science of The Total Environment* 482-483, 400-410.
Leland, A., Stanard, A., 2018. Light Duty PEMS Validations/Chassis Dynamometer Correlation, Coordinating Research Council (CRC), Prepared by the Eastern Research Group, Inc, Report: ERG No. 4043.00.001.001 Project E-122, p. 177.
Lelong J., 1999. Vehicle noise emission: evaluation of tyre/road-and motor-noise contributions, *International congress on noise control engineering*, Fort Lauderdale, Florida, USA.
Li, F., Lin, Y., Cai, M., Du, C., 2017. Dynamic simulation and characteristics analysis of traffic noise at roundabout and signalized intersections. *Applied Acoustics* 121, 14-24.
Liu, J., 2015. Driving Volatility in Instantaneous Driving Behaviors: Studies Using Large-Scale Trajectory Data. University of Tennessee.

Liu, S., Li, Q., Qiao, F., Du, J., Yu, L., 2017. Characterizing the Relationship between Carbon Dioxide Emissions and Vehicle Operating Modes on Roundabouts -A Pilot Test in a Single Lane Entry Roundabout. *Environment Pollution and Climate Change* 1(2), 1-120.

Luo, W.L., Cai, M., Li, F., Liu, J.K., 2012. Dynamic modeling of road traffic noise around buildings in an urban area. *Noise Control Engineering Journal* 60(4), 353-362.

Mahesh, S., Ramadurai, G., Shiva Nagendra, S.M., 2018. Real-world emissions of gaseous pollutants from diesel passenger cars using portable emission measurement systems. *Sustainable Cities and Society* 41, 104-113.

Makarewicz, R., Golebiewski, R., 2007. Modeling of the roundabout noise impact *The Journal of the Acoustical Society of America* 122(2), 860-868.

Makarewicz, R., Kokowski, P., 2007. Prediction of noise changes due to traffic speed control. *The Journal of the Acoustical Society of America* 122(4), 2074-2081.

Meneguzzer, C., Gastaldi, M., Arboretti Giancristofaro, R., 2018. Before-and-After Field Investigation of the Effects on Pollutant Emissions of Replacing a Signal-Controlled Road Intersection with a Roundabout. *Journal of Advanced Transportation* 2018, 15.

Meneguzzer, C., Gastaldi, M., Rossi, R., Gecchele, G., Prati, M.V., 2017. Comparison of exhaust emissions at intersections under traffic signal versus roundabout control using an instrumented vehicle. *Transportation Research Procedia* 25, 1597-1609.

Park, M., Lee, D., Park, J.-J., 2018. An Investigation of the Safety Performance of Roundabouts in Korea Based on a Random Parameters Count Model. *Journal of Advanced Transportation* 2018, 8.

Pouresmaeili, M.A., Aghayan, I., Taghizadeh, S.A., 2018. Development of Mashhad driving cycle for passenger car to model vehicle exhaust emissions calibrated using on-board measurements. *Sustainable Cities and Society* 36, 12-20.

Quartieri, J., Iannone, G., Guarnacci, C., 2010. On the Improvement of Statistical Traffic Noise Prediction Tools, *11th WSEAS Int. Conf. on Acoustics & Music: Theory & Applications*, Iasi, Romania, June 13-15, pp. 201-207.

Ramírez, A., Domínguez, E., 2013. Modeling urban traffic noise with stochastic and deterministic traffic models. *Applied Acoustics* 74(4), 614-621.

Rochat, J.L., Fleming, G.G., 2002. Validation of FHWA's traffic noise model (TNM): phase 1. United States. Federal Highway Administration.

Rodegerdts, L., Blogg, M., Wemple, E., Myers, E., Kyte, M., Dixon, M., List, G., Flannery, A., Troutbeck, R., Brilon, W., Wu, N., Persaud, B., Lyon, C., Harkey, D., Carter, D., 2007. Roundabouts in the United States, NCHRP 572, Transportation Research Board, Washington, DC.

Rodegerdts, L., Justin Bansen, Christopher Tiesler, Julia Knudsen, Edward Myers, Mark Johnson, Michael Moule, Bhagwant Persaud, Craig Lyon, Shauna Hallmark, Hillary Isebrands, R. Barry Crown, Bernard Guichet, Andrew O'Brien, 2010. Roundabouts: An Informational Guide - Second Edition.

Sakamoto, S., 2015. Road traffic noise prediction model ``ASJ RTN-Model 2013'': Report of the Research Committee on Road Traffic Noise. *Acoustical Science and Technology* 36(2), 49-108.

Salamati, K., Coelho, M.C., Fernandes, P.J., Rouphail, N.M., Frey, H.C., Bandeira, J., 2013. Emissions Estimation at Multilane Roundabouts: Effects of Movement and Approach Lane. *Transportation Research Record* 2389(1), 12-21.

Salamati, K., Rouphail, N.M., Frey, H.C., Liu, B., Schroeder, B.J., 2015. Simplified Method for Comparing Emissions in Roundabouts and at Signalized Intersections. *Transportation Research Record* 2517(1), 48-60.

Sandberg, U., 1987. Road traffic noise—The influence of the road surface and its characterization. *Applied Acoustics* 21(2), 97-118.
Sandhu, G., Frey, H., 2013. Effects of Errors on Vehicle Emission Rates from Portable Emissions Measurement Systems. *Transportation Research Record: Journal of the Transportation Research Board* 2340, 10-19.
To, W.M., Chan, T.M., 2000. The noise emitted from vehicles at roundabouts. *The Journal of the Acoustical Society of America* 107(5), 2760-2763.
Tutuianu, M., Bonnel, P., Ciuffo, B., Haniu, T., Ichikawa, N., Marotta, A., Pavlovic, J., Steven, H., 2015. Development of the World-wide harmonized Light duty Test Cycle (WLTC) and a possible pathway for its introduction in the European legislation. *Transportation Research Part D: Transport and Environment* 40, 61-75.
US EPA, 2002. Methodology for developing modal emission rates for EPA's multi-scale motor vehicle & equipment emission system.
Vasconcelos AL, Seco AM, Silva AB, 2013. Comparison of procedures to estimate critical headways at roundabouts. *Promet –Traffic&Transportation* 25(1), 43-53.
Vasconcelos, L., Silva, A.B., Seco, Á.M., Fernandes, P., Coelho, M.C., 2014. Turboroundabouts:Multicriterion Assessment of Intersection Capacity, Safety, and Emissions. *Transportation Research Record* 2402(1), 28-37.
Wang, H., Cai, M., Luo, W., 2017. Areawide dynamic traffic noise simulation in urban built-up area using beam tracing approach. *Sustainable Cities and Society* 30, 205-216.
WHO, 2016. Ambient air pollution: A global assessment of exposure and burden of disease World Health Organization, Retrieved from: https://www.who.int/phe/publications/air-pollution-global-assessment/en/, Accessed date: 18 November, 2019.
Yazdani Boroujeni, B., Frey, H.C., 2014. Road grade quantification based on global positioning system data obtained from real-world vehicle fuel use and emissions measurements. *Atmospheric Environment* 85, 179-186.
Yuan, M., Yin, C., Sun, Y., Chen, W., 2019a. Examining the associations between urban built environment and noise pollution in high-density high-rise urban areas: A case study in Wuhan, China. *Sustainable Cities and Society* 50, 101678.
Yuan, W., Frey, H.C., Wei, T., Rastogi, N., VanderGriend, S., Miller, D., Mattison, L., 2019b. Comparison of real-world vehicle fuel use and tailpipe emissions for gasoline-ethanol fuel blends. *Fuel* 249, 352-364.

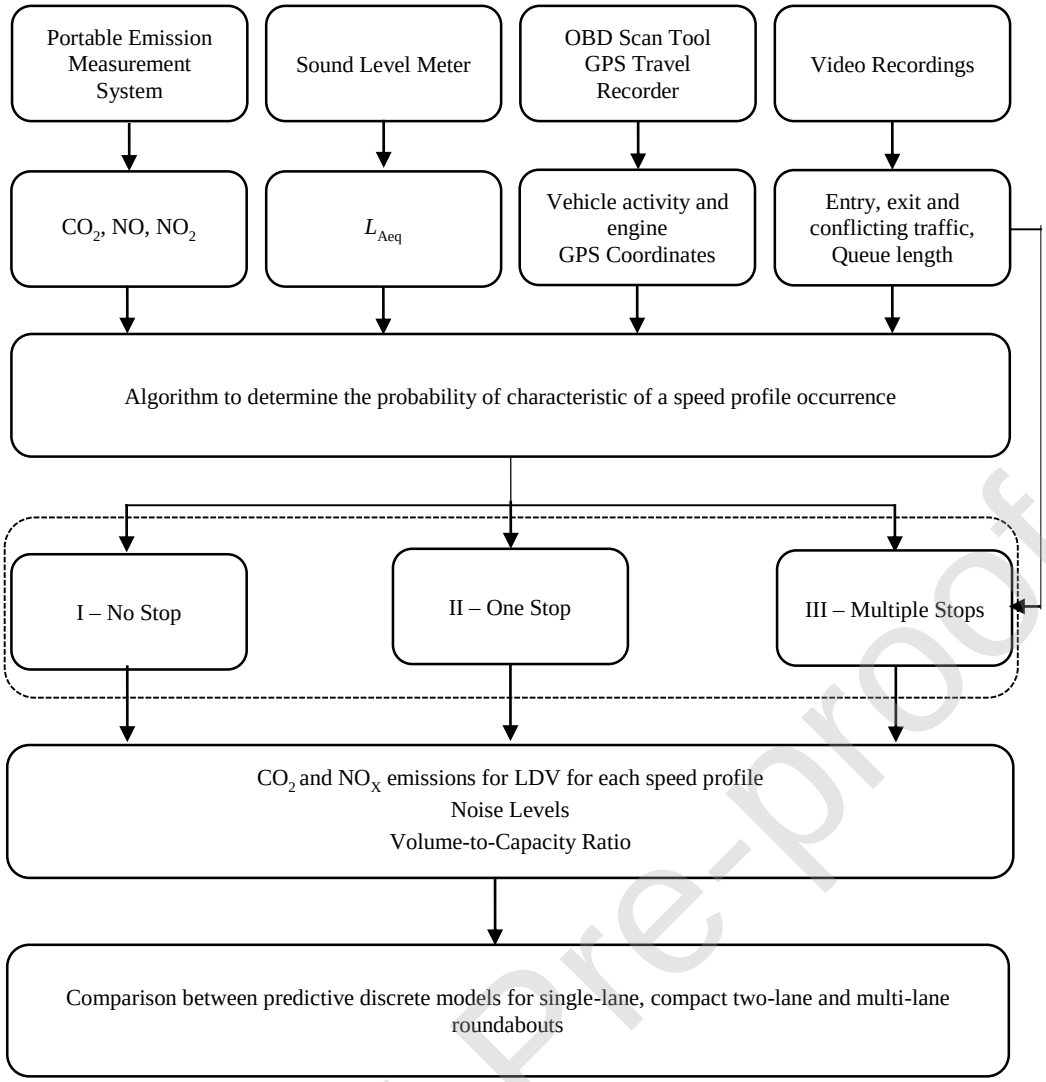

FIGURE 1 Methodology Overview

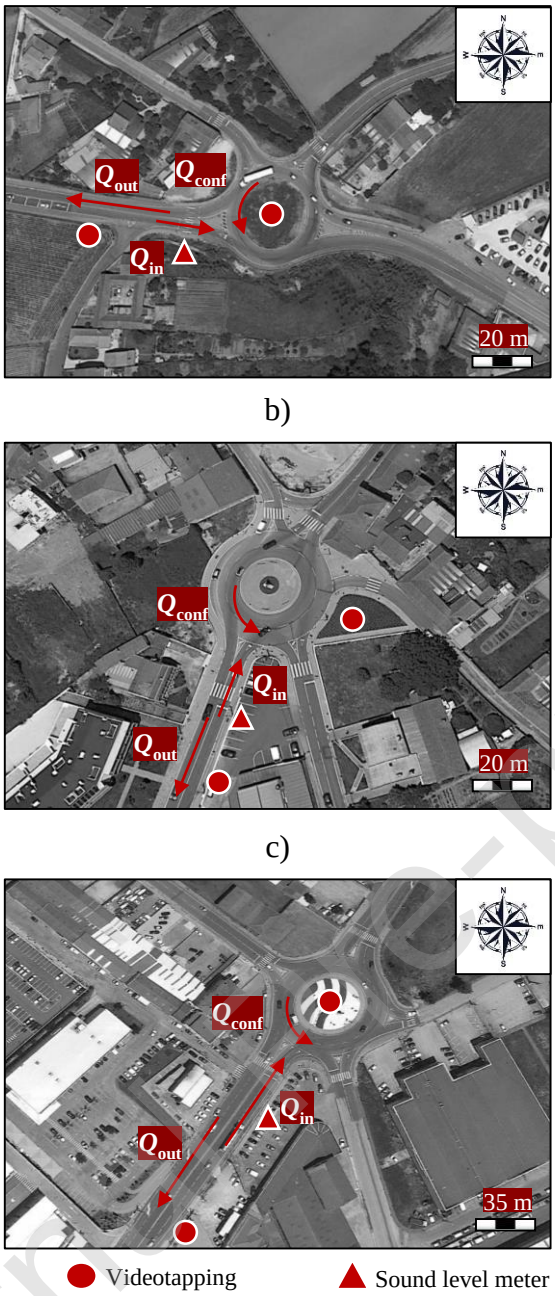

FIGURE 2 Aerial View of the three roundabouts, Aveiro, Portugal: a) SL; b) CTL; and c) ML

a)

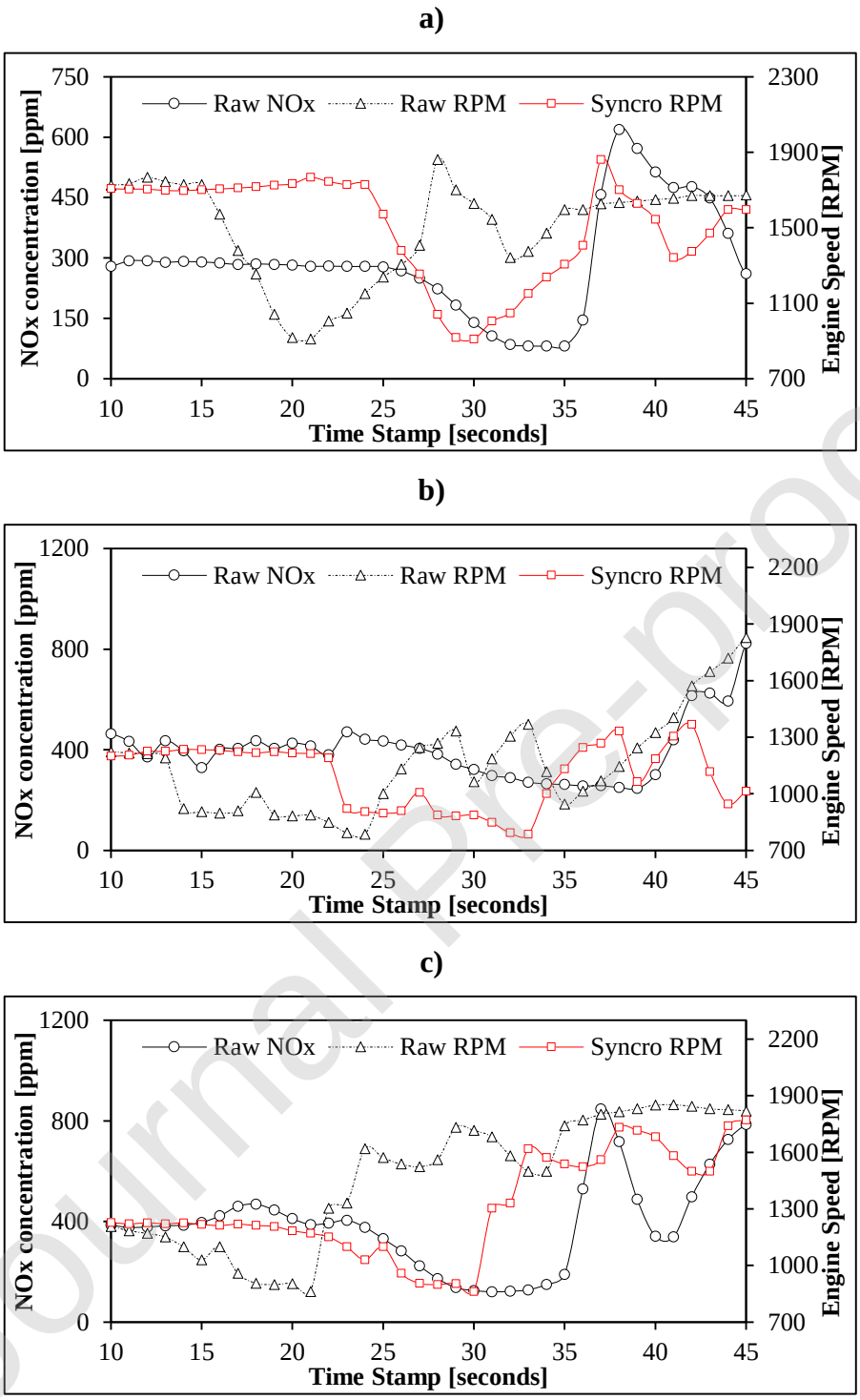

FIGURE 3 Synchronization of NOx versus RPM by roundabout layout: a) SL; b) CTL; and c) ML

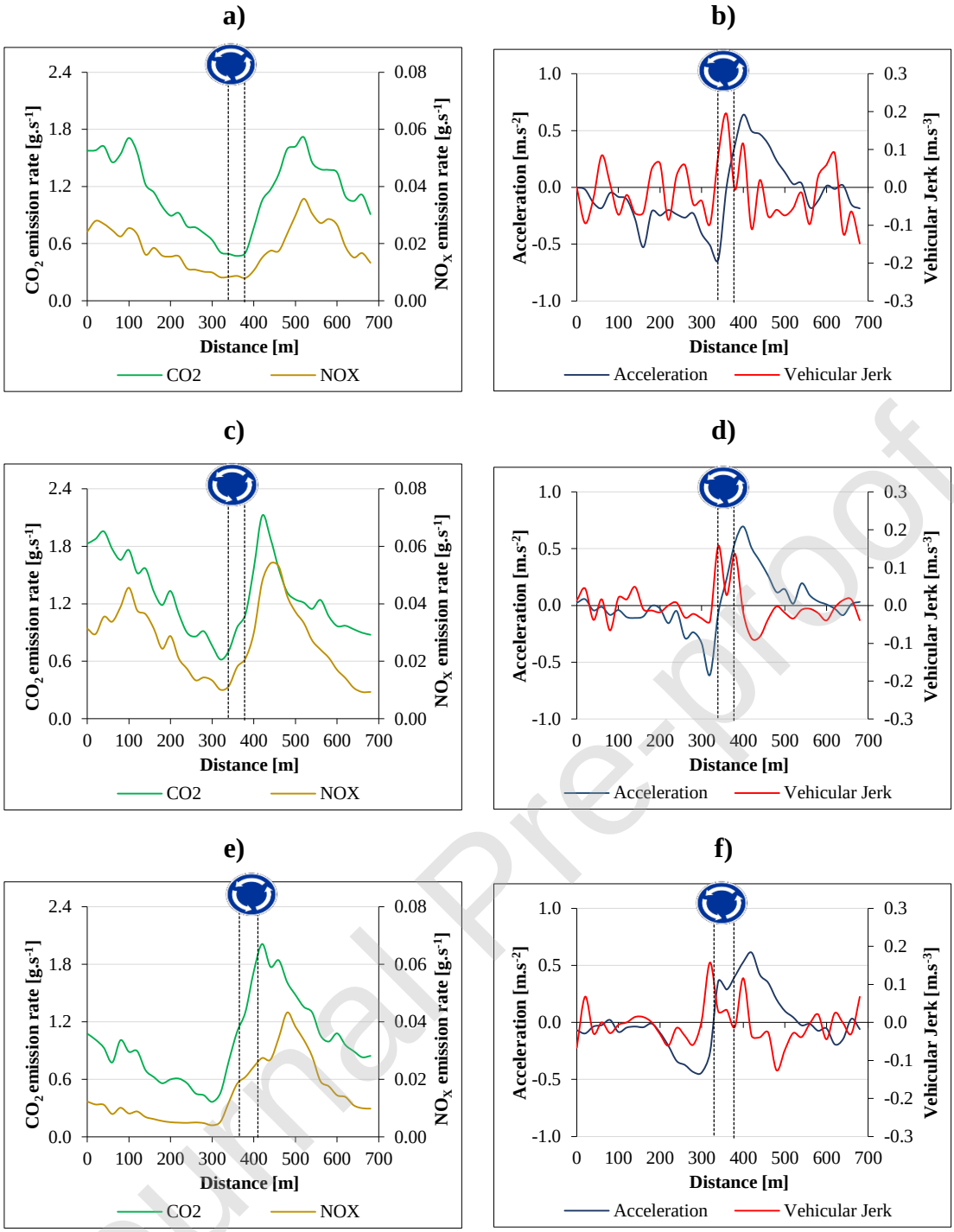

FIGURE 4 Measured parameters versus distance by layout: a) SL – CO_2/NO_X; b) SL – acceleration/ jerk; c) CTL – CO_2/NO_X; d) CTL – acceleration/jerk; e) ML – CO_2/NO_X; and f) ML – acceleration/ jerk

a)

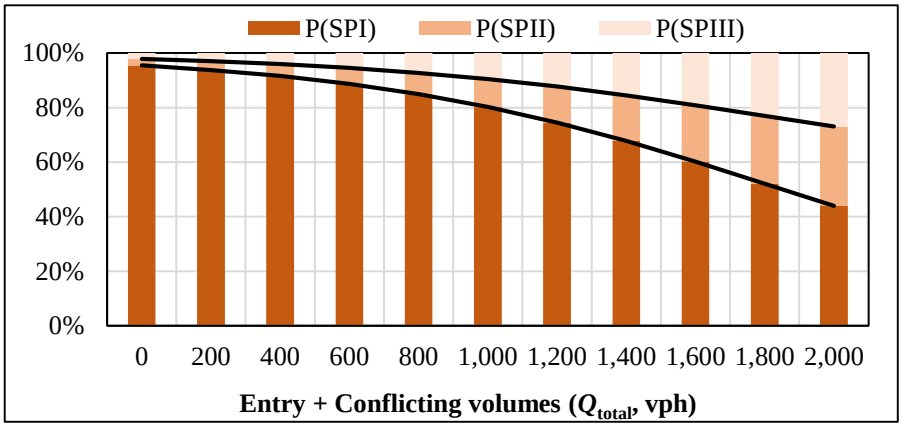

b)

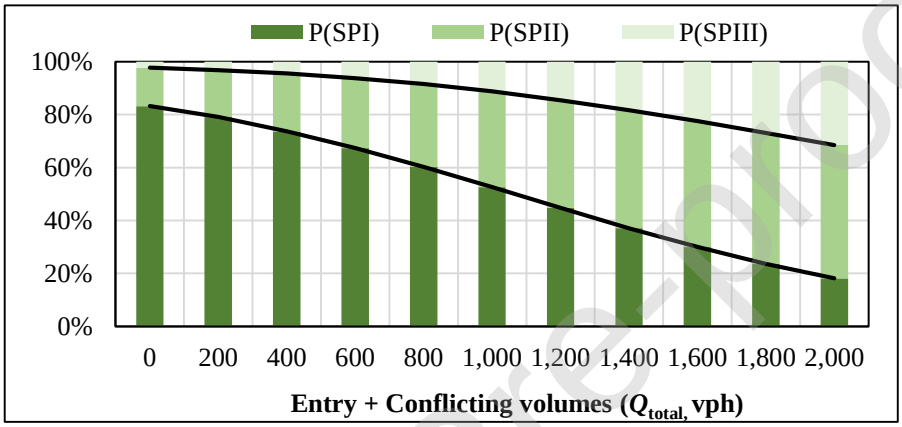

c)

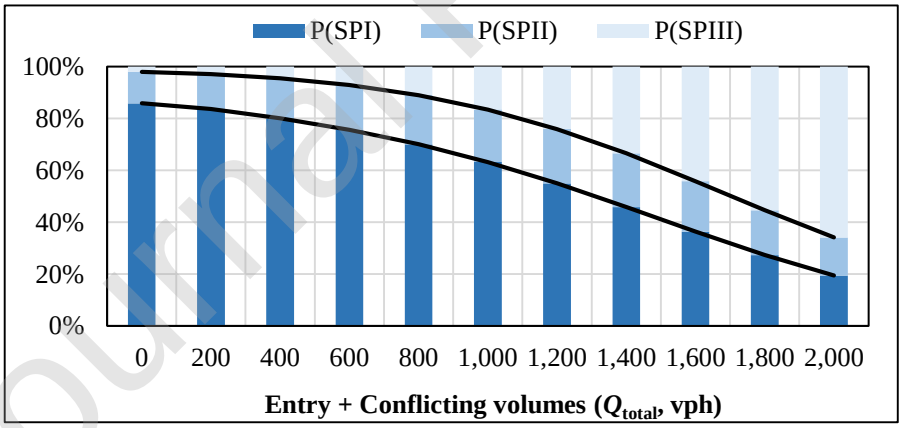

FIGURE 5 Predictive models for the relative occurrence of profiles I, II and III by roundabout layout: a) SL; b) CTL; and c) ML

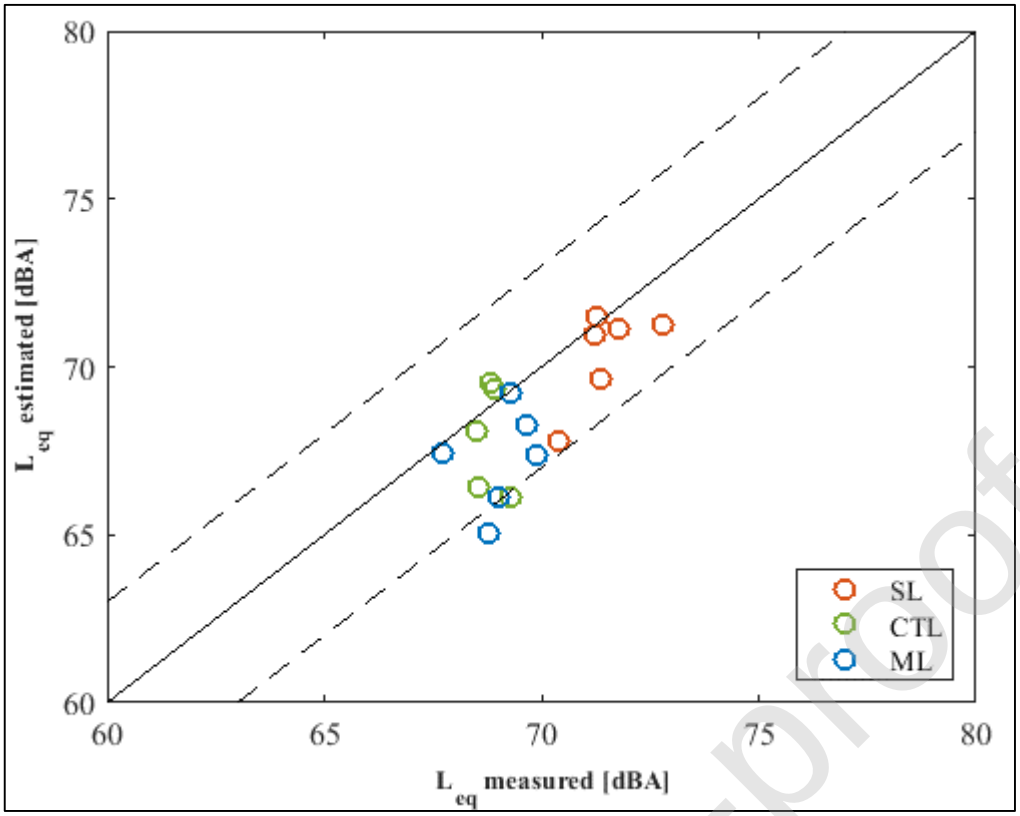

FIGURE 6 Noise model evaluation by roundabout layout

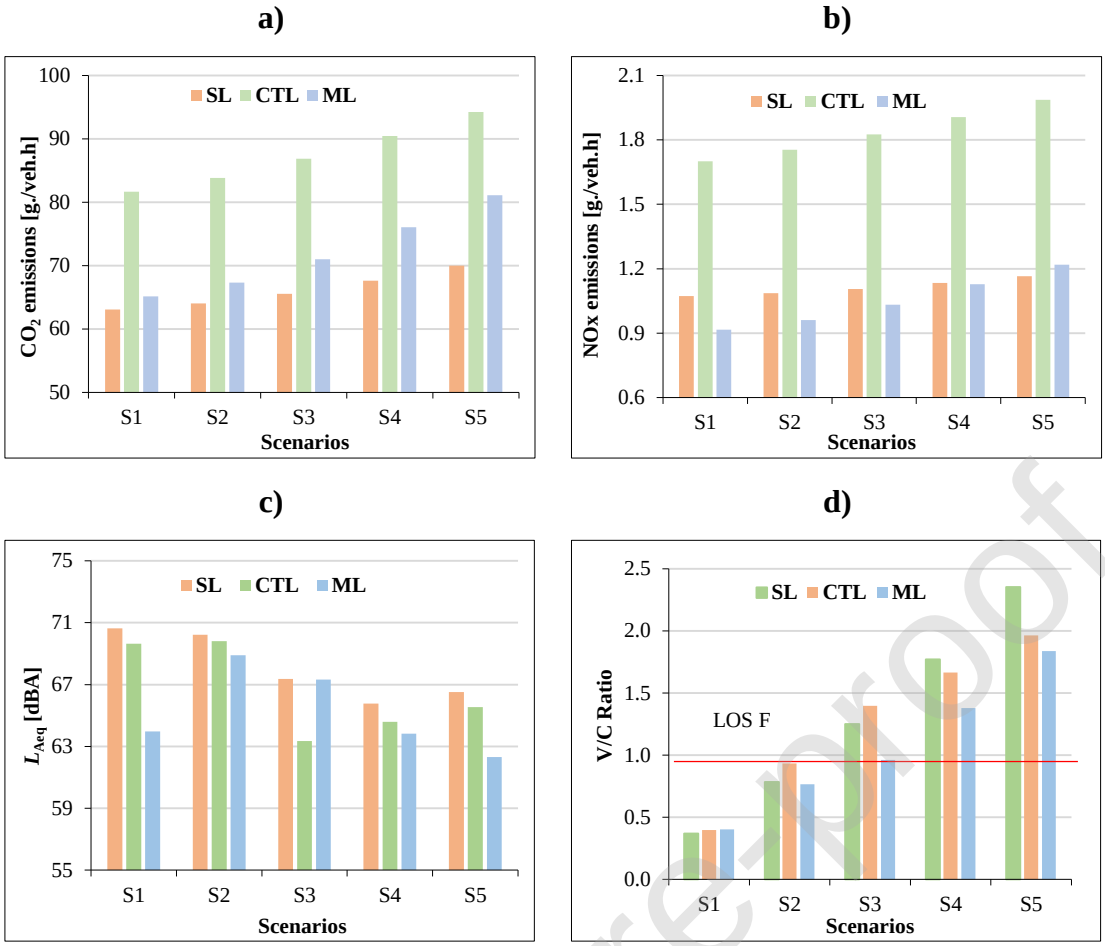

FIGURE 7 Variation of the measured parameters (hourly basis) by vehicle and scenario: a) CO_2; b) NO_x; c) L_{eq}; and d) V/C

TABLE 1 Geometric and operational for the three roundabout data collection sites

ID	Entering Speed ($km.h^{-1}$)	Circulating Speed ($km.h^{-1}$)	Circulating Width (m)	ICD (m)	Central Island (m)	Q_{in} + Q_{out} (vph)	Heavy Duty Vehicles (%)
SL	58.6	28.8	6	44	32	700 – 1,700	~10%
CTL	44.5	24.2	9.5	36	18	300 – 1,400	~2%
ML	40.1	29.2	10	55	35	700 – 2,200	~5%

TABLE 2 Average traffic performance and emissions (with standard deviation values) by speed profile and roundabout layout

ID	Speed Profile	RPA (m/s^2)	Travel Time (s)	Idle Time (s)	CO_2 (g/km)	NOx (g/km)
SL	I	0.18 (0.07)	58 (7)	N/A	92 (14)	1.56 (0.96)
	II	0.22 (0.05)	67 (6)	3.4 (2.4)	103 (20)	1.28 (0.56)
	III	0.23 (0.04)	78 (9)	5.7 (1.9)	122 (5)	2.44 (0.72)
	Average	0.19 (0.07)	68 (7)	4.5 (2.1)	105 (13)	1.76 (0.75)
CTL	I	0.16 (0.05)	61 (5)	N/A	114 (11)	2.35 (0.68)
	II	0.18 (0.03)	67 (5)	2.9 (1.3)	123 (23)	2.67 (1.13)
	III	0.22 (0.03)	112 (36)	14.8 (9.8)	171 (35)	3.54 (1.42)
	Average	0.18 (0.05)	80 (15)	8.8 (5.5)	136 (23)	2.85 (1.07)
ML	I	0.16 (0.03)	67 (10	N/A	90 (14)	1.23 (0.48)
	II	0.20 (0.03)	71 (7)	3.1 (1.7)	110 (14)	1.75 (0.48)
	III	0.22 (0.06)	97 (17)	21.0 (12.5)	129 (21)	1.95 (0.70)
	Average	0.17 (0.04)	78 (11)	12.1 (7.1)	110 (16)	1.64 (0.55)

Note: N/A = Not Applicable

TABLE 3 Trip driving classification by speed profile and roundabout layout

ID	Speed Profile	Speeding (% time)		Acceleration (% time)			Vehicular jerk (% time)	RPA (% trips)	
		$v_i > v_{max}$	$v_i > 1.1 \times v_{max}$	$a < -3.4$	$a > a_i^+$	$a > 2.16$	$j > 0.9$	RPA > 0.12	RPA > 0.14
SL	I	11.0 (17.1)	5.8 (12.7)	0.3 (0.9)	29.1 (7.9)	0.5 (1.2)	5.5 (4.3)	71	65
	II	7.0 (8.2)	3.4 (6.7)	0.2 (0.8)	32.6 (6.2)	1.5 (1.4)	9.3 (6.4)	100	100
	III	6.1 (4.4)	0.7 (1.0)	2.0 (0.9)	35.1 (7.9)	1.8 (1.4)	10.8 (2.4)	100	100
	All trips	10.0 (15.6)	5.1 (11.6)	0.4 (1.0)	30.1 (7.9)	0.8 (1.3)	6.5 (5.0)	78	73
CTL	I	11.8 (11.1)	5.7 (12.2)	0.4 (1.1)	33.9 (8.7)	0.3 (1.2)	4.4 (6.5)	92	53
	II	11.1 (10.7)	1.3 (12.2)	1.2 (0.8)	37.1 (9.5)	1.5 (0.6)	10.2 (3.3)	100	96
	III	6.6 (8.0)	1.3 (3.3)	1.1 (1.0)	37.5 (5.9)	0.8 (1.5)	2.7 (3.0)	100	100
	All trips	11.4 (15.0)	3.5 (9.3)	0.8 (1.0)	35.6 (8.6)	0.8 (1.1)	6.2 (3.8)	96	76
ML	I	11.1 (12.2)	2.1 (5.0)	1.2 (2.9)	30.5 (7.2)	1.4 (3.5)	5.9 (7.1)	90	71
	II	11.3 (16.7)	4.5 (11.1)	2.5 (4.1)	32.6 (6.8)	4.1 (5.0)	11.3 (8.8)	100	100
	III	2.9 (4.0)	0.5 (0.9)	5.7 (7.0)	32.7 (11.0)	8.8 (9.4)	15.6 (12.1)	100	100
	All trips	10.1 (13.6)	2.7 (7.6)	2.3 (4.3)	31.5 (7.8)	3.4 (5.7)	9.1 (9.2)	95	85

Note: N/A = values in parentheses represent the standard deviation values when applicable

TABLE 4 Calibrated β parameters applied in the multinomial logistic regression model to obtain P_{SPII} and P_{SPIII}

ID	Probability of Speed Profile	Parameter	β	Std. Error	Wald test	*p*-value
SL	P_{SPII}	Intercept	-3.711	0.220	283.824	<0.0001
		Q_{total}	0.020	0.000	61.358	<0.0001
	P_{SPIII}	Intercept	-3.788	0.265	204.379	<0.0001
		Q_{total}	0.002	0.000	24.135	<0.0001
CTL	P_{SPII}	Intercept	-1.746	0.147	141.075	<0.0001
		Q_{total}	0.002	0.000	64.766	<0.0001
	P_{SPIII}	Intercept	-3.599	0.254	200.899	<0.0001
		Q_{total}	0.003	0.000	57.275	<0.0001
ML	P_{SPII}	Intercept	-1.954	0.147	175.930	<0.0001
		Q_{total}	0.001	0.000	83.454	<0.0001
	P_{SPIII}	Intercept	-3.789	0.188	404.415	<0.0001
		Q_{total}	0.003	0.000	279.951	<0.0001

The parameters were statistically significant at the 1%,5% and 10% significance level (p-value < 0.01, p-value < 0.05, and p-value < 0.10).